

Stratigraphy, sedimentology and eruptive mechanisms in the tuff cone of El Golfo (Lanzarote, Canary Islands)

Dario Pedrazzi · Joan Martí · Adelina Geyer

Received: 4 September 2012 / Accepted: 10 June 2013 / Published online: 3 July 2013
© Springer-Verlag Berlin Heidelberg 2013

Abstract The tuff cone of El Golfo on the western coast of Lanzarote (Canary Islands) is a typical hydrovolcanic edifice. Along with other edifices of the same age, it was constructed along a fracture oriented NEE–SWW that coincides with the main structural trend of recent volcanism in this part of the island. We conducted a detailed stratigraphic study of the succession of deposits present in this tuff cone and here interpret them in light of the depositional processes and eruptive dynamics that we were able to infer. The eruptive sequence is represented by a succession of pyroclastic deposits, most of which were emplaced by flow, plus a number of air-fall deposits and ballistic blocks and bombs. We distinguished five different eruptive/depositional stages on the basis of differences in inferred current flow regimes and fragmentation efficiencies represented by the resulting deposits; the different stages may be related to variations in the explosive energy. Eight lithofacies were identified based on sedimentary discontinuities, grain size, components, variations in primary laminations and bedforms. The volcanic edifice was constructed very rapidly around the vent, and this is inferred to have controlled the amount of water that was able to enter the eruption conduit. The sedimentological characteristics of the deposits and the nature and distribution of palagonitic alteration suggest that most of the pyroclastic succession in El Golfo was deposited in a subaerial environment. This type of hydrovolcanic explosive activity is common in the coastal zones of Lanzarote and the other Canary Islands and is one of the main potential hazards that could threaten the human population of this archipelago. Detailed studies of these hydrovolcanic eruptions such as the one we

present here can help volcanologists understand the hazards that this type of eruption can generate and provide essential information for undertaking risk assessment in similar volcanic environments.

Keywords El Golfo · Lanzarote · Canary Islands · Tuff cone · Hydrovolcanism · Facies analysis

Introduction

Hydrovolcanism is a volcanic phenomenon in which magma or magmatic heat interacts with an external source of water (Macdonald 1972; Sheridan and Wohletz 1981). Typically, it takes place in deep or shallow submarine, littoral, lacustrine, phreatic or subglacial environments. Common volcanic landforms produced by hydrovolcanic eruptions include tuff cones, tuff rings and maar-diatreme volcanoes. Varieties of landforms are attributable to differences in eruption intensities, in styles of explosions and in depositional processes (Sheridan and Wohletz 1983). These differences are determined by variables such as the exact nature of the magma and water involved, the proportions and properties of the interacting fluids, the lithology and mechanical properties of the rocks of the conduit wall, and vent geometry (Kokelaar 1986; Sohn and Chough 1989; Sohn 1996; White 1996; White and Houghton 2000; White and Ross 2011). Also of importance is the geometry of the water-to-magma interface. Due in some cases to their short duration and often remote location, these hydrovolcanic eruptions have only ever been observed or documented on a few occasions in places such as Myojin, Japan (Morimoto 1960), Surtsey, Iceland (Thorarinsson 1965), Taal, Philippines (Moore et al. 1966), Capelinhos, Faial Island, Azores (Machado et al. 1962; Cole et al. 2001), Ukinrek, Alaska (Kienle et al. 1980; Self et al. 1980), Karymskoye Lake, Kamchatka (Belousov and Belousova 2001), Kavachi, Solomon Islands (Baker et al.

Editorial responsibility: T. Thordarson

D. Pedrazzi (✉) · J. Martí · A. Geyer
Group of Volcanology, SIMGEO (UB-CSIC) Institute of Earth
Sciences Jaume Almera, c/Lluis Sole Sabaris s/n,
08028 Barcelona, Spain
e-mail: dpedrazzi@ictja.csic.es

2002), Katla eruptions (Larsen et al. 2009; Larsen 2010), Grimsvotn, Iceland (Jude-Eton et al. 2012; IMO/IES websites, Iceland) and Eyjafjallajökull, Iceland (Gudmundsson et al. 2012).

Hydrovolcanic eruptions are common in coastal environments where erupting magma is prone to interact with seawater in either subaquatic or subaerial settings depending on the location of the eruption conduit and vent (Sheridan and Wohletz 1983). Water may gain access to magma either in the subsurface as groundwater or at the surface, and water entry is controlled largely by the exact nature of the rocks enveloping the vent site and eruption-related. Near-shore and shallow subaqueous activity may generate high-intensity explosions characterised by ballistic blocks, ash fall and pyroclastic density currents that can represent a hazard for nearby population centres. This is a threat above all on volcanic islands where basaltic magmas, which can erupt relatively passively under magmatic conditions, may become highly explosive when interacting with seawater in coastal environments (Moore et al. 1966; Waters and Fisher 1971; Sumner 1998; Cole et al. 2001; Baker et al. 2002; Sohn et al. 2003; Cronin et al. 2006; Clark et al. 2009; Németh and Cronin 2009, 2011).

Although examples of basaltic hydrovolcanic eruptions can be found on all the Canary Islands in the form of maars and tuff cones and rings, very few have ever been studied in detail. Published studies include those of include Montaña Amarilla, Montaña Escachada and Caldera del Rei on Tenerife (De La Nuez et al. 1993), Bandama on Gran Canaria (Araña et al. 1988), La Palma's 1949 eruption (White and Schmincke 1999) and Montaña Los Erales on Tenerife (Clark et al. 2009). Canarian hydrovolcanic events include both inland phreatomagmatic eruptions generated by erupting magmas interacting with groundwater and surtseyan eruptions caused by the interaction of magma with water in coastal or shallow offshore settings.

In the present paper, we study the tuff cone of El Golfo, located on the west coast of Lanzarote and a very typical of Canarian hydrovolcanic coastal edifice (Fig. 1). Our main objective was to describe in detail the structure and association of the facies in an archetypal tuff cone and use this information to infer changes in eruption style and depositional processes applicable to tuff cones worldwide. In the case of El Golfo, eruption of the basaltic magma was modified by interaction with seawater, and the eruptive sequence is characterised by a simple pyroclastic succession. In order to identify and characterise the different eruptive phases and pulses that constructed El Golfo, we here (1) describe the stratigraphy of the succession of deposits, (2) analyse their lithological and sedimentological characteristics, and (3) interpret these deposits in terms of the depositional regime and the efficiency of the magma fragmentation, which in turn are used to infer changes in the eruption dynamics and the degree of the magma-to-water interaction (Wohletz and

Sheridan 1983). Finally, we discuss the implications for human settlements on Lanzarote of the hazards that are inherent in this type of eruption.

Geological setting and general description of the tuff cone of El Golfo

The Canary Islands are a group of seven large islands and several islets that form a 450-km-long archipelago located 100 km off the northwest coast of Africa (Fig. 1). They were constructed by volcanic and tectonic activities that started at around 60 Ma ago and continue to the present day (Robertson and Stillman 1979; Le Bas et al. 1986; Marinoni and Pasquarè 1994; Marinoni and Gudmundsson 2000).

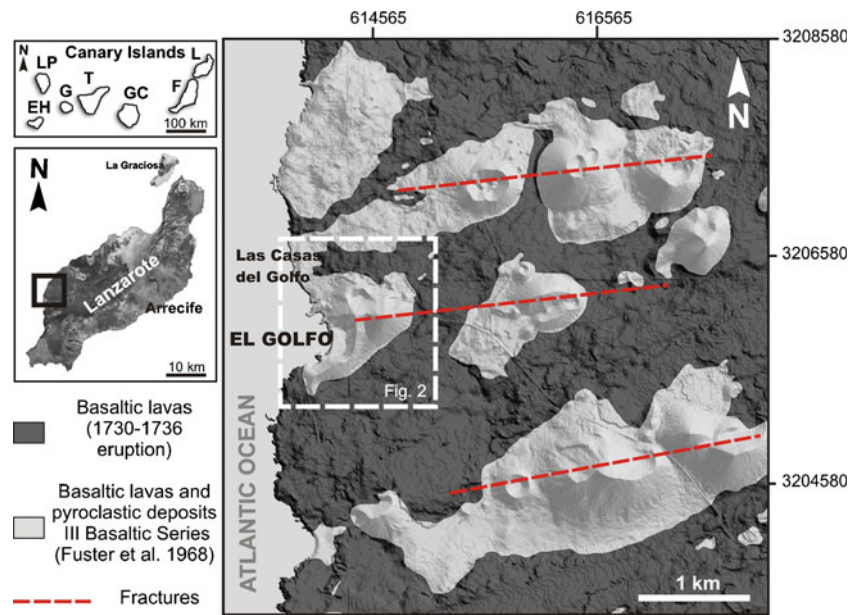
Lanzarote is the north easternmost of the Canary Islands (Fig. 1). It represents the emergent part of the East Canary Ridge, a NNE–SSW linear volcanic structure located on typical oceanic crust that is at least 11 km thick (Banda et al. 1981). The shallow basement of the island is probably about 4–5 km thick (Banda et al. 1981) and is composed of sedimentary (quartzite and shales), plutonic (basic and ultrabasic) and subvolcanic rocks (basaltic and trachytic dikes). The erupted magma contains an abundance of quartzite and sandstone xenoliths (Araña and Carracedo 1978). Although the island's lavas are almost all basaltic, there are small outcrops of massive trachytes in the oldest parts of the island (NW and SE).

The volcanic stratigraphy of Lanzarote was first classified by Fuster et al. (1968) as having four eruptive series: (I) a tableland with basalts dated at 6–12 Ma (Miocene–Pliocene); (II–III) Quaternary volcanism dated at 1 Ma and separated from stage I by an erosional unconformity; and (IV) recent volcanism including the 1730–1736 eruption, the largest eruption in modern times on the Canary Islands.

Marinoni and Pasquarè (1994) divided the geological evolution of the emergent part of Lanzarote into two principal construction stages named the 'Pre-erosional or Shield stage' and the 'Post-erosional or Differentiated stage'. The main volcanostratigraphic units of the former stage are exposed locally on the west coast of the island and correspond to scoriaceous lavas of basaltic composition and subordinate trachytic intrusions, scoria and tuff cones, as well as lavas of basaltic composition. The post-erosional Quaternary stage is characterised mainly by aligned scoria cones and associated lava flows.

The volcanic edifice of El Golfo, located on the western coast of Lanzarote (Fig. 1), reaches 60 m a.s.l. and has a basal diameter of approximately 1 km, which gives it an aspect ratio of about 0.05. The volcanic edifice has been partially destroyed by marine erosion, and only its eastern part remains intact. The age of this volcano is not well known, but it is assumed to be a product of recent volcanism on the island (since 2 Ma) (Abdel-Monem et al. 1972).

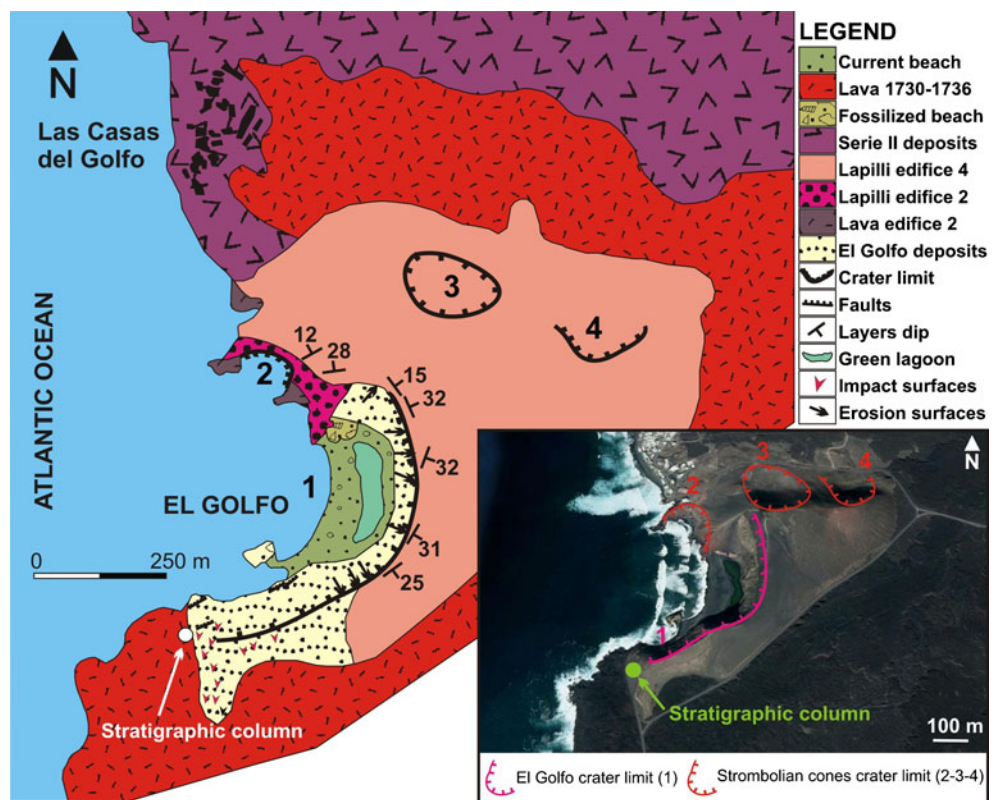
Fig. 1 Location and simplified geological map of the study area: *EH* El Hierro, *F* Fuerteventura, *G* Gomera, *GC* Gran Canaria, *L* Lanzarote, *LP* La Palma, *T* Tenerife



A simplified geological map of El Golfo is given in Fig. 2. Its deposits are covered by the lavas that were generated by the 1730–1736 event. El Golfo, together with other edifices of the same age, forms a linear vent system running NEE–SWW that coincides with the main orientation of recent volcanism in this part of the island (Marinoni and Pasquare 1994), whose products, today eroded by wave action, partially cover the area of El Golfo.

The tuff cone consists entirely of a succession of pyroclastic deposits with different lithological and sedimentological characteristics. The composition of its juvenile fragments is homogeneous which are of poorly evolved intraplate alkali basalt that does not vary through the whole eruptive sequence (Martí and Colombo 1990). The pyroclasts are rich in olivine and pyroxene phenocrysts, which are enclosed within the glassy groundmasses of the pyroclasts. A number of lapilli

Fig. 2 Geological map of the tuff cone of El Golfo (modified from Martí and Colombo 1990) from a Google Earth image of the volcanic edifice showing the main crater (1), the three subsequent craters (2–3–4) located to the north of the volcanic edifice, and the location of the studied stratigraphic sequence



are highly vesicular (>70 % vesicles) and have a very low density (<1 g/cm³); nevertheless, their mineralogical and chemical compositions do not differ from those of the other, denser, juvenile pyroclasts. Dunite and gabbro xenoliths ranging in size from 5–30 cm are common (Fig. 3). An irregularly distributed palagonitic alteration of the juvenile vitric fragments, which were devitrified and transformed into smectites, zeolites (mainly phillipsite) and Fe oxides, is another distinctive feature of the deposits on El Golfo (Martí and Colombo 1990) (Fig. 4).

Methods

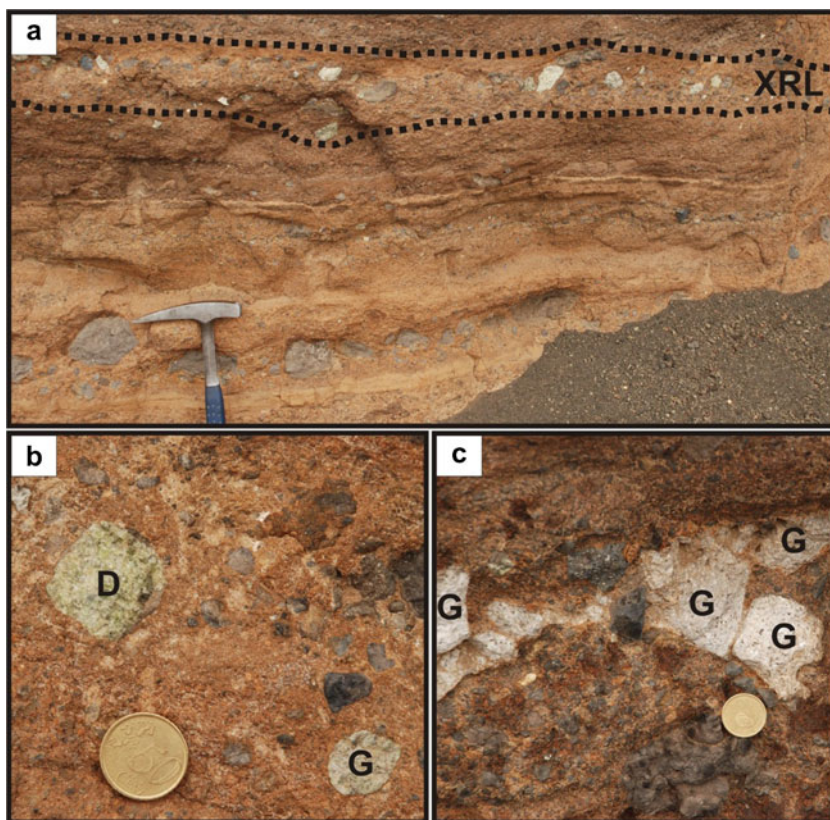
The research we present here is above all the result of new fieldwork. An investigation was carried out in order to establish the relationships between the different volcanic edifices present in an area 2 km² around El Golfo. Relative ages were determined on the basis of stratigraphic correlations. Detailed field measurements of the succession were then conducted on the main outcrop located in the southern part of the edifice (Fig. 2). Unfortunately, access to the other parts of the cone for close observation is impossible. Our studies included bed-by-bed thickness measurements of the deposits and facies analysis. Deposits were divided into lithofacies (Table 1) based on different criteria (see below) and following the facies model and nomenclature proposed by Chough

and Sohn (1990) and Solgevik et al. (2007). Due to the post-depositional palagonitisation that affects an important part of the sequence, it was not possible to obtain samples for mechanical sieving in the laboratory. Therefore, grain size determinations for the >64 mm fraction were performed partially in the field using grain size comparators. The grain size of clasts smaller than 64 mm was determined from thin sections using image analysis techniques (e.g., ImageJ software). The grain size classification is modified after Chough and Sohn (1990) due to field conditions and comprises ash <2 mm, fine lapilli = 2–8 mm; medium lapilli = 8–32 mm and coarse lapilli = 32–64 mm. Bed thickness is based on Ingram (1954): lamina (<1 cm); very thin bed (1–3 cm), thin bed (3–10 cm), medium bed (10–30 cm), thick bed (30–100 cm) or very thick bed (>100 cm). Scanning electron microscopy data for juvenile particles were taken from Martí and Colombo (1990).

Facies description

The tuff cone of El Golfo stands at sea level and has a well-exposed 45-m-thick stratigraphic section that exhibits differences in the size and shape of the clasts, in the levels of alteration and in the depositional features. We grouped the cone's deposits into eight facies and facies associations based on the following criteria: (1) sedimentary discontinuities such as erosion surfaces, (2) variations in grain size and percentage

Fig. 3 Field photographs of: **a** detail of the deposits in which the levels with gabbro and dunite xenoliths are visible (XRL); **b** detail of dunite (D) and gabbro (G) xenoliths; **c** detail of gabbro (G) xenoliths



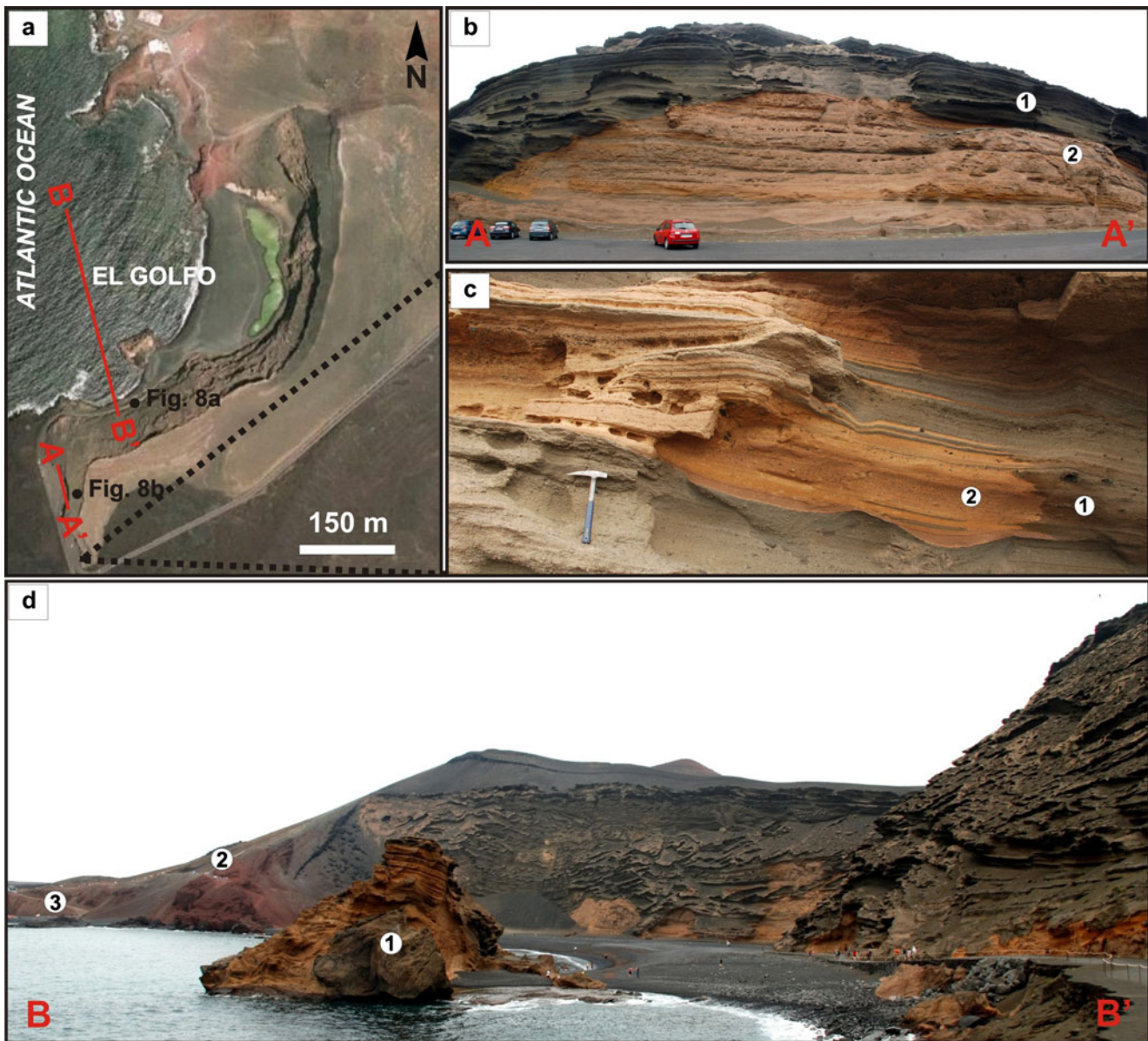


Fig. 4 **a** Google Earth image of the volcanic edifice of El Golfo; **b** field photographs of a NNW–SSE cross-section of the deposit sequence at El Golfo (*A–A'*); **c** detail of the deposits, where both the non-altered deposits (*1*) and the palagonitised deposits (*2*) are visible. Note the irregularity of the limit between the altered and non-altered zones that

is independent of the current topographical surface; **d** field photograph of El Golfo showing (*1*) the fallen block of the tuff cone in the present-day beach and (*2* and *3*) the Strombolian deposits (posterior to the emplacement of the tuff cone) located to the northeast (*B–B'*)

of volcanic bombs and (*3*) variations in primary bedforms. Erosion surfaces constitute the main discontinuity between deposits but only affect specific levels, the rest of the stratigraphic column being depositionally continuous (Fig. 5).

Channel fill facies (*A*)

This facies consists predominantly of thin structureless beds of juvenile and lithic clasts (Fig. 6a). Juvenile ash and medium lapilli fragments are rounded, dense and non-vesicular. Juvenile vesicular ballistic fragments (up to 3 cm) occur on

specific levels. Angular lithic fragments of lavas and xenoliths (up to 3 cm) can be found alongside accretionary lapilli of 1 cm. The average size of matrix grains is about 2 mm. The coarsest lithic fragments tend to be concentrated in the lowest part of the deposits. This facies is present mainly as fillings of depressions and occurs as lenses (maximum depth of 0.5 m and width of 0.4 m) (Fig. 7a–c) or in V- or U-shaped channels (depth of 1.5 m with a maximum width of 2 m) (Fig. 7d). The bedding planes are marked by sharp variation in grain size. Individual beds are generally ungraded and have irregular and erosive boundaries.

Table 1 Lithofacies and lithofacies association

Units	Lithofacies associations	Lithofacies	Interpretation
I	G1	B E	High rate of direct suspension sedimentation that alternate with tractional deposition (depending on the deposition rate)
II	G2	D E	Upper flow-regime bedforms
III	G3	A C E	A Erosive initial phase with a following depositional stage C–E Deposition of turbulent pyroclastic surges fluctuating in velocity and particle concentration with episodes of high shear stress
IV	G4	A D G H	A Eroding current with erosive surfaces with larger size than G3 D–G–H Multiple pyroclastic surges with “wet” hydromagmatic explosion
V	G5	D E F G H	Continuous changing conditions of the surge with possible moderate amount of liquid water

Letters indicate the different lithofacies: *A* channel-fill facies, *B* massive crudely stratified facies, *C* diffusely stratified facies, *D* stratified facies, *E* undulate ash-bed facies, *F* dune facies, *G* antidune facies and *H* accretionary lapilli facies

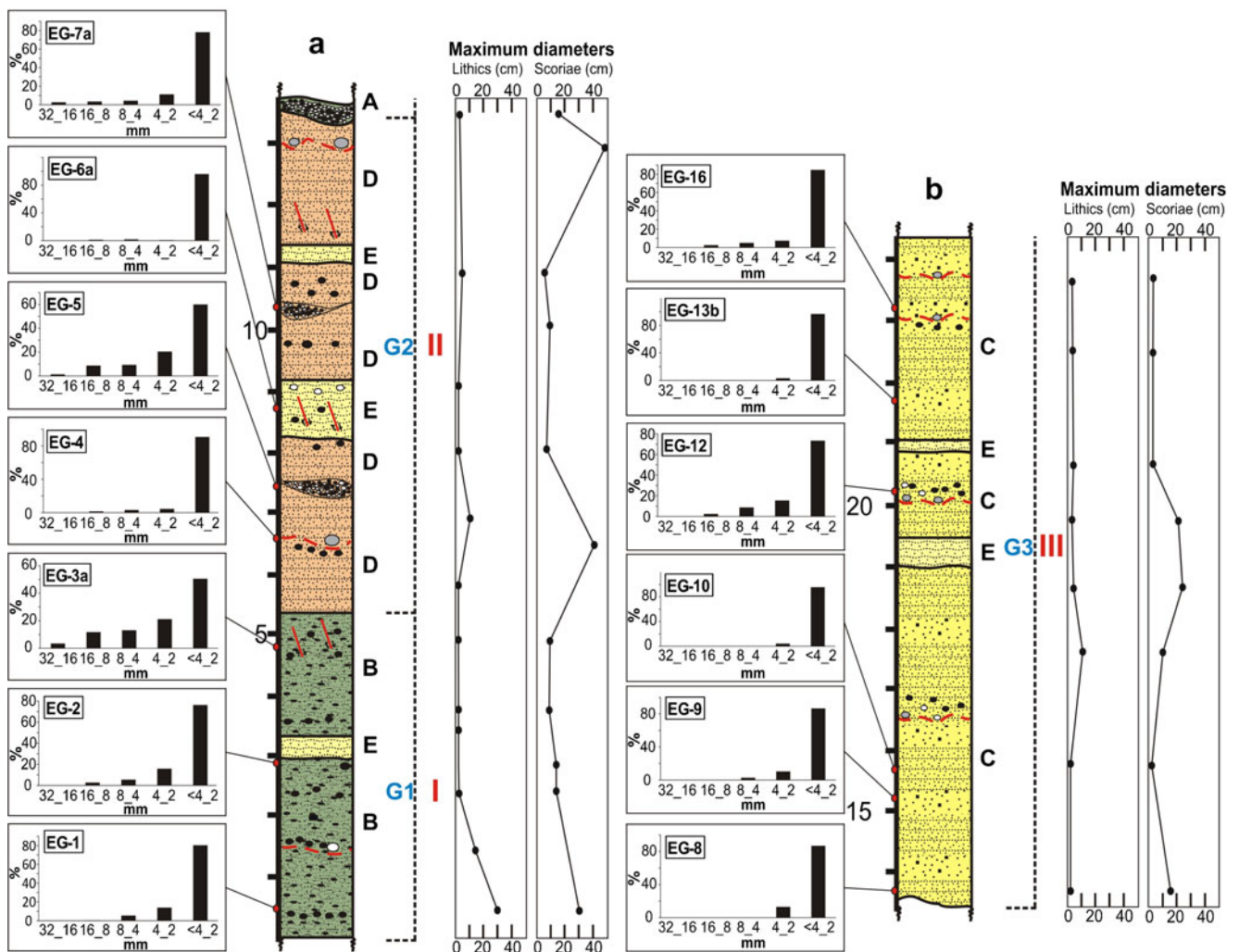


Fig. 5 Composite stratigraphic column of the deposits at El Golfo showing the main facies: **a** channel fill facies, **b** crudely stratified facies, **c** diffusely stratified facies, **d** planar stratified facies, **e** undulate ash-bed facies, **f** dune facies, **g** antidune facies and **h** accretionary lapilli facies.

Five stages (I–V) are identified based on the depositional processes and resulting deposits. Vertical variations in grain size and the maximum diameter of lithics and scoriae clasts are also indicated

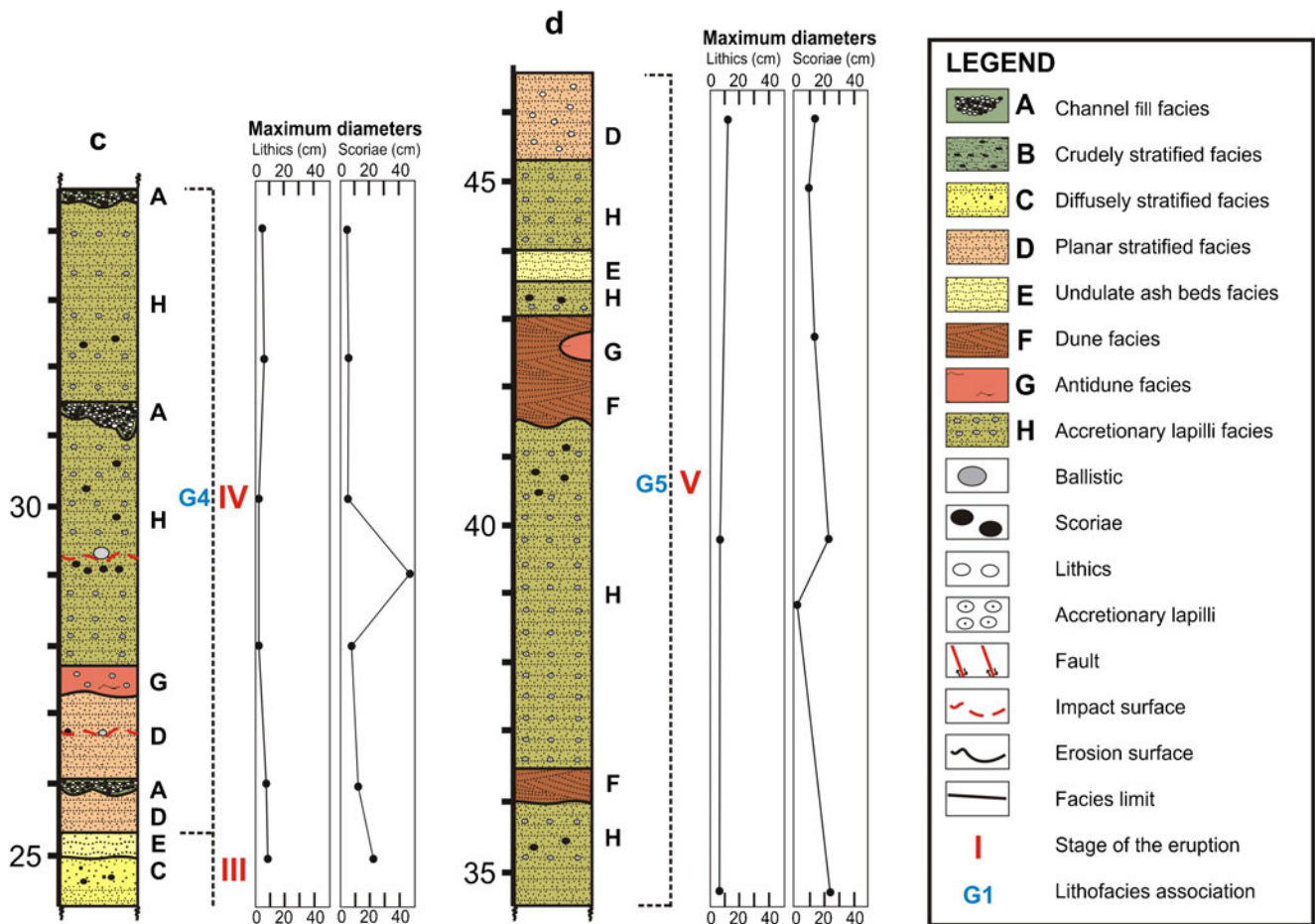


Fig. 5 (continued)

Crudely stratified facies (B)

This facies has a maximum thickness of 3 m (Fig. 5) with crude thin to medium beds (Fig. 6b). It consists of clast-supported layers, with subrounded, poorly vesicular juvenile coarse-to-medium lapilli with ballistic ejecta (up to 30 cm) in a matrix of fine lapilli and coarse ash (EG1; EG2; EG3A: Fig. 5). The fragment population in this facies is dominantly juvenile. However, many of the ballistic blocks are accidental basaltic fragments. The crude layering in this facies is defined by the presence of thick-bedded packets containing several indistinct and discontinuous boundaries with about 10–30 cm vertical spacing. Overall, the sequences are laterally continuous with single beds pinching and swelling laterally, and grading that varies vertically from normal to reverse.

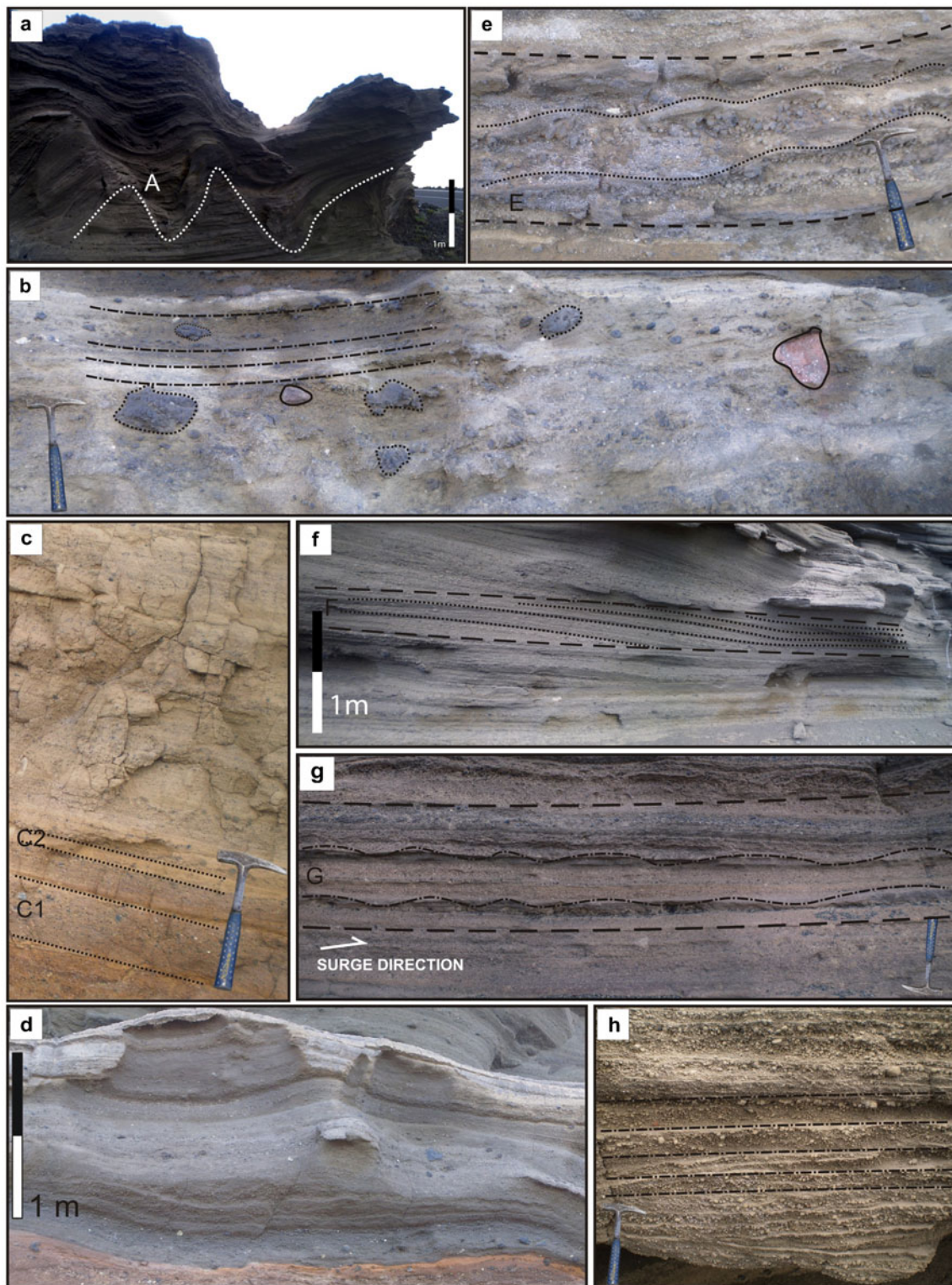
Diffusely stratified facies (C)

This facies has a maximum thickness of 5 m (range, 1–5 m) (Fig. 5) and consists of alternating ash and lapilli beds (Fig. 6c). The juvenile fine lapilli are rounded and non-vesicular. The matrix is palagonitised basaltic ash with crystal fragments of olivine and clinopyroxene. In a few levels

(often in the middle of the deposits), there is a significant increase in the number of bombs and blocks (plutonic xenoliths). Bombs can be up to 35 cm in size, while blocks are no larger than 20 cm. This facies is characterised by a visually obvious separation between layers. It consists of laterally continuous beds where, on the one hand, poorly sorted fine, lapilli-rich massive layers with a coarse ash matrix (EG9; EG13B; EG16: Fig. 5) and thicknesses ranging from a few centimetres to several decimetres thick alternate with, on the other hand, a coarse ash matrix and well-sorted ash-rich layers (EG8; EG10: Fig. 5) with thin laminations.

Planar stratified facies (D)

This facies is represented by a set of up to 2-m-thick homogeneous planar (Fig. 5) and laterally continuous multiple layers moderately sorted with bedding planes plus internal planar laminations (Fig. 6d). Juvenile fine lapilli are commonly subangular and non-vesicular. The coarse fraction (up to 10 cm) consists of lava fragments and poorly vesicular juvenile ballistic scoria bombs, with somewhat fewer xenolith fragments (max 3–5 cm). The matrix is made up of palagonitised basaltic ash with crystal fragments of olivine



and clinopyroxene. Planar lamination is locally visible in the less palagonitised layers; otherwise, the matrix appears generally to be massive due to textural modification by alteration. Typically, the contact below each bed is well-defined and non-erosive. Ballistic fragments up to 50 cm can be

found. Individual beds are thin (1–5 cm) and vary from fine lapilli-rich beds to ash and exhibit good sorting with both normal and reverse grading. Some levels are characterised by poorly sorted deposits (EG5; EG7a; Fig. 5) with coarse and medium lapilli in a matrix of fine lapilli and coarse ash that

Fig. 6 Field photographs of the characteristic facies at the tuff cone of El Golfo: **a** channel-fill facies made of heterogeneous bedded ash and lapilli. Individual beds are generally ungraded with irregular and erosive boundaries. The *dashed white line* indicates the erosion surface; **b** massive crudely stratified facies including a thin- to medium-bedded, massive to crudely stratified unit (*dotted-dashed line*). It is also possible to distinguish the ballistic clasts corresponding to accidental basaltic fragments (*continuous line*) and bombs (*dotted line*); **c** diffusely stratified facies with continuous beds (C1) of poorly sorted lapilli-rich layers alternating with (C2) lapilli-poor layers with a yellow ash matrix; **d** planar stratified facies composed of planar and laterally continuous beds with internal stratification. This facies can be distinguished from the diffusely stratified facies because this has continuous lateral planar bedding with constant moderately sorted layers 2–3 cm and better sorting in each bed; **e** undulate ash-bed facies consisting of laterally continuous, well-sorted ash and lapilli beds with pinch-and-swell structures and undulate laminations (*dotted line*); **f** dune facies with crests up to 40 cm and sets with foresets dipping downstream migrating downstream (*dotted line*); **g** antidune facies with crest (*dotted-dash line*) up to 40 cm height with a wavelength of 15 cm; **h** accretionary lapilli facies commonly containing cores of coarse ash and fine lapilli. Individual plane-beds (*dotted-dash line*) alternate from fine lapilli-rich to ash-rich layers

fill in the small depressions. Despite resembling a diffusely stratified facies, this planar stratified facies is distinguished by the presence of continuous lateral planar bedding with constant moderately sorted layers of 2–3 cm and better sorting of each bed.

Undulate ash bed facies (E)

This facies, with a maximum detected thickness of just a few decimetres (Fig. 5), is represented by laterally continuous, well-sorted ash beds alternating with fine lapilli beds (EG6a: Fig. 5), which have undulate laminations and pinch-and-swell structures (Fig. 6e). Crests can be up to 5 cm in height and wavelengths vary from 5 to 10 cm. Some beds display brittle rupture due to the impact of ballistic ejecta.

Dune facies (F)

This facies is only present in the upper part of the succession at El Golfo. It has a maximum thickness of 1.5 m (Fig. 5) and forms large dunes (Fig. 6f). These can be up to 40 cm in height, and their wavelengths vary from 1.5 to 2 m. Individual thin beds are generally moderately sorted, structureless or reversely graded. The coarse fraction consists of juvenile medium lapilli, accretionary lapilli up to 1 cm and accidental lithic fragments (up to 4 cm) that are basaltic in nature with a matrix of coarse ash. The laminae are defined by a clast-supported fabric from which all fine material has disappeared. In front of these structures, the foresets (maximum length 50 cm) are well-preserved and exhibit clear sigmoidal geometry. Both the top and bottom set laminations are still observable, the latter asymptotic to the basal bedding plane (Fig. 6f). These dunes are similar to the ones described as Type A by Cole (1991).

Antidune facies (G)

This facies, with a maximum thickness of a few decimetres (Fig. 5), consists of small bedforms with stoss sides preserved (Fig. 6g). These deposits are generally moderately sorted with individual beds alternating between juvenile fine lapilli-rich and ash-rich and loose accretionary lapilli with a maximum size of 1 cm. Crests are up to 15 cm in height with a wavelength of 40 cm (Fig. 5).

Accretionary lapilli facies (H)

This facies is only found in the upper part of the sequence, where it has a maximum thickness of 5 m (Fig. 5) and represents a level of mainly accretionary lapilli (Fig. 6h). Although present in small amounts in other facies, the accretionary lapilli are mostly concentrated in this level. They commonly contain cores of juvenile coarse ash and fine lapilli with coarser clasts up to about 3 cm in size and are defined as rim type (Schumacher and Schmincke 1991, 1995). Deposits are usually moderately sorted, showing planar and laterally continuous beds with internal lamination. Individual plane beds are 5 cm thick and alternate between fine lapilli-rich and ash-rich layers.

Facies associations

We distinguished five lithofacies associations between the base and the top of the succession at El Golfo (Fig. 5, Table 1). As we explain below (see “Discussion”), these facies associations can be correlated to the different stages in the eruption that constructed the volcanic edifice on the basis of, on the one hand, the physical appearance of the deposits that make up the succession and, on the other, the differences in the inferred fragmentation, transportation and deposition mechanisms.

The first lithofacies association (G1) (stage I; Fig. 5) is represented by deposits exposed at sea level, mainly correspond to crudely stratified facies alternating with a small proportion of undulate ash-bed facies. Both of these facies are clearly characterised by juvenile clasts with accidental basaltic ballistic fragments, as well as notable differences in the distribution of the grain size of the deposits (Fig. 5). This lithofacies association represents the lowest part of the volcanic sequence at El Golfo (Fig. 5). The second lithofacies association (G2) (stage II; Fig. 5) exhibits a gradual transition from the previous stage and has planar stratified facies with minor undulate ash-bed facies. These deposits are finer-grained, planar and laterally continuous with episodes with undulate beds. Both facies are characterised by impact lithics of basalt. The following lithofacies association (G3) (stage III; Fig. 5) is characterised by an abrupt change, and deposits

are present mainly as fillings of depressions and as lenses (channel-fill facies). As the construction of the edifice progressed, deposits became progressively more poorly sorted: Massive lapilli-rich facies alternate with deposits characterised by well-sorted lapilli-poor, thinly bedded, internally stratified (diffuse stratified deposits) and, to a lesser extent, undulate facies. Accidental fragments (basaltic and xenoliths) characterise specific levels of the lithofacies (Fig. 5). This lithofacies association corresponds to the mid-part of the volcanic sequence. The next facies association (G4) (stage IV; Fig. 5) is characterised by a transitional change to planar stratified facies, accretionary lapilli and antidune facies, all followed by abundant lenses and V- and U-shaped channels associated with larger-sized channel-fill facies than those in G3. The final stage (G5) (stage V; Fig. 5) produced dunes and antidunes and accretionary lapilli, along with undulate and planar stratified facies. This lithofacies association is the uppermost in the depositional sequence and reveals an important change in the bedforms: Dunes and antidunes predominate, with a decrease in the average grain size of the matrix from fine lapilli/coarse ash to coarse-fine ash.

Discussion

Facies interpretation

Based on the stratigraphic and geological features discussed in this study, the volcano of El Golfo is revealed as a tuff cone constructed close to the shoreline mainly by deposition from pyroclastic surges and emplacement of minor ballistic blocks and bombs. The interpretation of the lithofacies and the lithofacies associations identified in this study provides the necessary clues for understanding the eruption, transport and depositional mechanisms involved in the construction of the volcanic edifice of El Golfo. A channel-fill facies (A) consists of beds confined to channels formed by an eroding current with an erosive initial phase followed by a depositional stage. Massive muddy ash and lapilli lenses (Fig. 6a) can be interpreted as volcanoclastic water-logged gravity currents (Cas and Wright 1987) based on the observed clearly defined boundaries and massive fine ash appearance. These geometries are in fact replaced in the lower part of the facies by massive deposits (Fig. 7a). In some cases, it is possible to infer that a two-stage process filled these channels (Fig. 7b–c): first of all, erosion by a passing current generated the V-shaped geometries that were subsequently coated by a thin veneer of fine ash deposited presumably by an ash-rich current through the channels (Fisher 1977; Verwoerd and Chevallier 1987); secondly, the channels were completely filled in by the materials transported the later pyroclastic surges. In other cases such as the U- and V-

shaped rills (Fig. 7d), the erosive surfaces are larger and were probably formed by surface runoff from flows after the deposition of the pyroclastic material. Erosional features in surge deposits are well documented (e.g. Moore 1967; Fisher 1977; Kieffer and Sturtevant 1986). As proposed in Wohletz (1998), the two-phase flow behaviour of a surge is influenced by topographic variability and implies particle deposition in cases of subsonic surges or erosion in supersonic surges.

As suggested by Valentine (1987), for any given stratified flow encountering an obstacle, there will be a level (streamline) above which all fluid has sufficient energy to surpass the obstacle and below which all fluid either is stopped (blocked) or simply moves around the obstacle with no upward motion. This critical level is referred to as the 'dividing streamline'. An increasing Rouse number, that is, the ratio of particle settling velocity to the scale of turbulence (Middleton and Southard 1978), due possibly to the confinement of the surge, causes lower parts to become dense enough to assume the characteristics of a pyroclastic flow. This leads to the deposition of the characteristic facies observed at El Golfo, where the deposits tend to have a massive fine ash appearance, and the coarsest lithics tend to be found in the lowest part of the deposits.

As suggested by Solgevik et al. (2007) for the Capelas tuff cone (Sao Miguel Island, Azores), crudely stratified facies (B) (Fig. 6b) might be the result of a rapid emplacement from a high concentration boundary layer with weak tractional transport. Alternatively (in the case of more pronounced tractional transport), this facies might be interpreted as deposits from a traction carpet in a highly concentrated boundary layer. The presence of blocks and bombs is indicative of ballistically emplaced ejecta.

The diffusely stratified facies (C) is characterised by a visible difference in grain size and sorting between the lapilli and ash-rich layers (Fig. 6c) and could be interpreted as the result of either an unsteady pyroclastic surge or multiple, closely spaced events (Dellino et al. 2004a). Poorly sorted, lapilli-rich, massive layers with crude associated stratification might be the result of rapid deposition from suspension with little traction, whereas well-sorted lapilli-poor layers with thin internal laminations could be indicative of a relatively slow deposition rate resulting in grain segregation (Arnott and Hand 1989).

In the planar stratified facies (D), it is difficult to discriminate the depositional mechanisms due to a lack of outcrops. Planar lamination, sometimes visible in the less palagonitised layers (Fig. 6d), could suggest that the facies was the product of a pyroclastic surge in which a single couplet consisting of fine lapilli and ash-grade beds was formed by a single surge (Sohn and Chough 1989; Dellino et al. 2004a, b).

The undulate ash beds (E) can be interpreted as pyroclastic surge deposits primarily on the basis of the low-angle cross

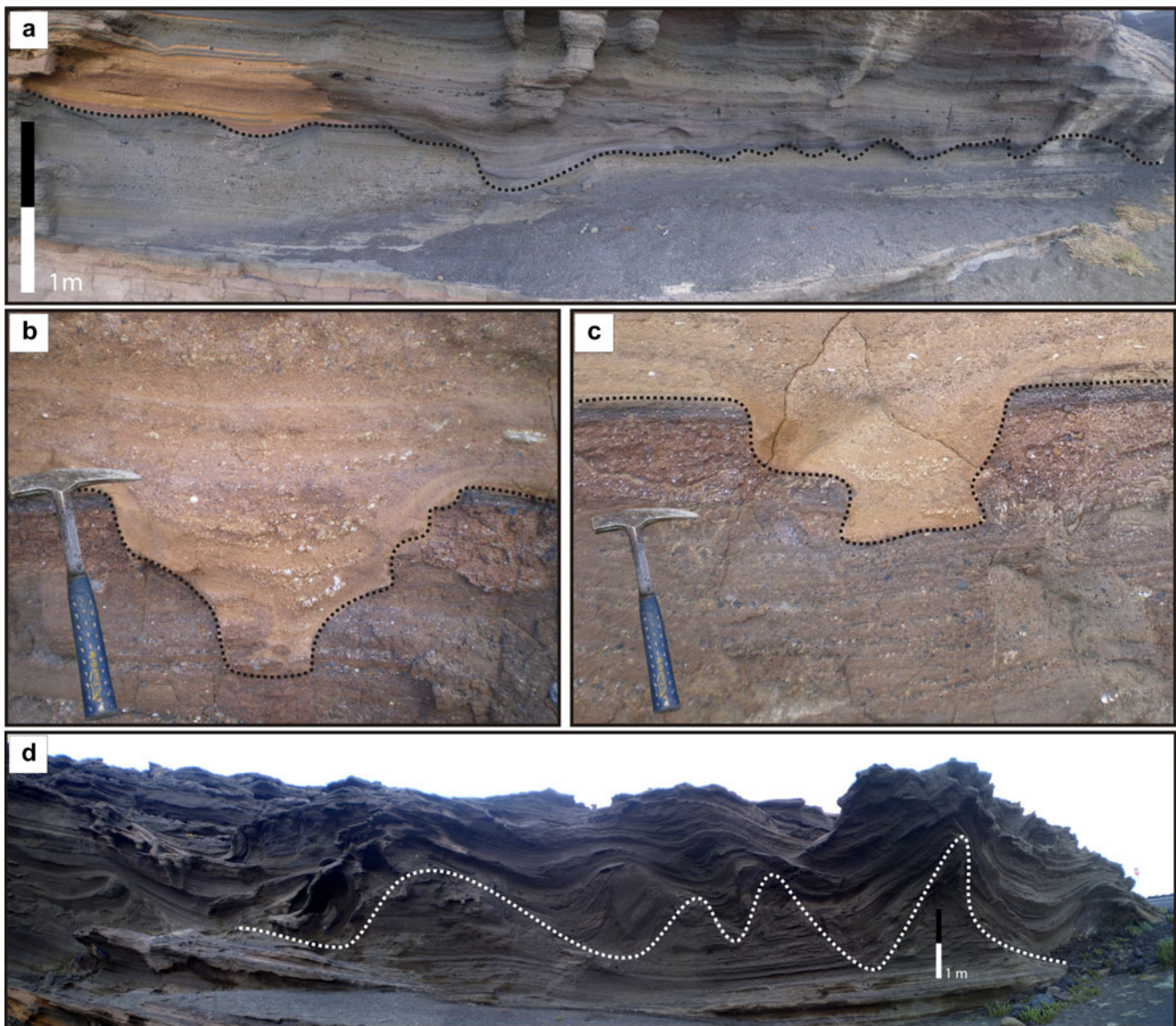


Fig. 7 Field details of channel-fill facies: **a** V-shaped geometry (*dotted line*) and crudely stratified replenishment of the erosion cavities excavated in plane beds by pyroclastic surge deposits; **b c** channels filled in two stages: First, the flow generated the V-shaped geometries (*dotted line*) that were subsequently coated by the massive dense flows that circulated

through the channels. Finally, the materials transported by the latter pyroclastic surges replenished the cavities; **d** U- and V-shaped rill geometries (*white dotted line*). The erosive surfaces have larger geometries and are thought to have been formed by surface runoff from flows after the deposition of the pyroclastic material

lamination. The existence of these structures (Fig. 6e) may be the result of variations in the flow regime (Valentine and Fisher 2000) and in particle concentration (Sohn and Chough 1989; Sohn 1996). Given the relationship between flow regimes and resulting bedforms (Cas and Wright 1987), low-angle undulate ash-beds with weak stratification could be interpreted as the result of a low-flow regime, thereby indicating a decreasing velocity of the flow or lower to transitional regime produced by a relatively low concentration pyroclastic surge.

Aside from undulate ash-beds, the dune facies (F) (Fig. 6f) are classified as lower-flow-regime bedforms (Cas and Wright 1987). Fisher and Schmincke (1984) argued that sand-wave migration direction is controlled by velocity and flow regime,

and a similar situation was proposed by Druitt (1992) for the May, 1980, Mount St. Helens blast deposits: regressive sand waves (antidunes) formed where the blast was accelerating and progressive sand waves (dunes) where it was decelerating.

The antidune facies (G) (Fig. 6g) occurs where there is supercritical flow (Cas and Wright 1987). The presence of accretionary lapilli might indicate that the corresponding pyroclastic surges were wet (i.e. they consisted of three-phase flows with gas, particles and liquid water), as suggested by Lorenz (1974a, 1974b), Walker (1984) and Sohn and Chough (1992).

Accretionary lapilli facies (H) (Fig. 6h) commonly form in steam-rich hydrovolcanic eruption columns (Self and Sparks 1978) or in convecting pyroclastic surge clouds when solid

particles pick up sticky wet ash (Waite and Dzurisin 1981). During the lateral spreading of surges, particles form core agglomerate due to accidental collisions and when the binding forces of liquid bridges from condensed moisture exceed the grain-dispersive forces (Schumacher and Schmincke 1995).

The depositional characteristics of the pyroclastic surge deposits at El Golfo and the absence of secondary reworking by sea waves suggest that the emplacement of the deposits and the construction of the cone occurred in a subaerial environment. In addition, the irregular distribution of palagonitic alteration indicate that, given the depositional characteristics of the deposits, the palagonitisation was produced in a subaerial environment, as suggested by Martí and Colombo (1990).

Most of the pyroclastic deposits in the edifice consist of a fine-grained matrix embedding coarse scoria, lithic fragments and volcanic bombs and blocks (emplaced ballistically) (Figs. 6 and 8), which suggests that the transportation process of this pyroclastic material was not able to develop any proper grain-sorting process. The lack of clear fallout deposits is a remarkable feature of the succession at El Golfo. This, together with lithological and depositional features such as ripples, dunes, antidunes and tabular forms, as well as the circular distribution of deposits, indicates that most pyroclastic deposits formed from turbulent, highly dilute pyroclastic surges (see Druitt 1998; Freundt and Bursik 1998; Huppert 1998; Branney and Kokelaar 2002) expanding radially from the eruptive vent. In fact, variations in vertical facies are usually

related to variable rates of energy release occurring during an ongoing eruption (Sohn and Chough 1989). The apparent lack of fallout deposits may be interpreted either as a direct consequence of the eruption dynamics (i.e. absence of fallout mechanisms in proximal areas) or of their erosion and assimilation by the pyroclastic surges.

Eruptive dynamics

Along with accretionary lapilli and accidental lithics, particles with morphology and textures related to hydromagmatic fragmentation (block-like shapes, low vesicularity, presence of adhered dust, tephra size and superficial chemical alteration) (Martí and Colombo 1990) dominate the deposits found in the tuff cone of El Golfo. The dynamics of hydrovolcanism are controlled by the complex thermodynamics of magma–water interaction, which determines the nature of explosive activity, and are characterised by variable energy outputs and different degrees of magmatic or hydromagmatic fragmentation (Wohletz and Sheridan 1983; Houghton and Hackett 1984; Kokelaar 1986; White and Houghton 2000; Mastin et al. 2004). Depending on the extent of the magma–water interaction and the modes of transport and deposition, hydrovolcanic deposits show remarkable variability in between-layer and within-layer. The efficiency of hydromagmatic fragmentation and the corresponding eruption dynamics are controlled by magma viscosity, temperature, the pressure differences between magma

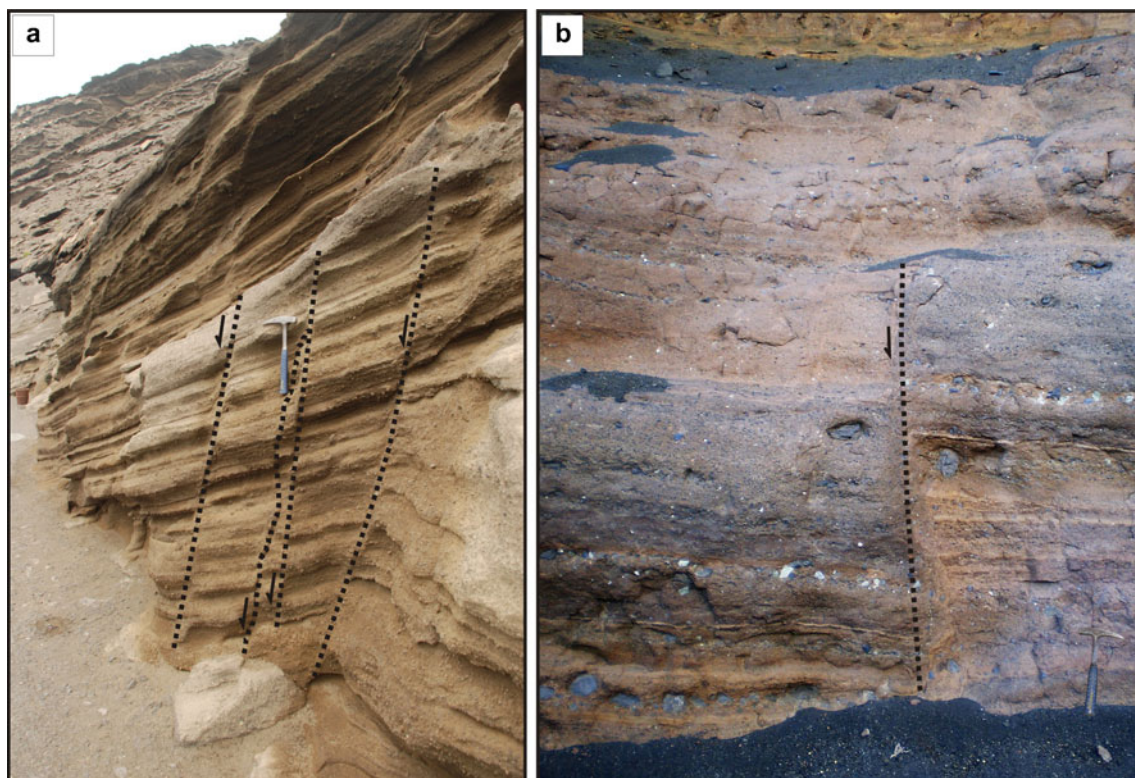


Fig. 8 Field photographs showing examples of subvertical settlement faults existing around the edifice

and water, and the water/magma contact mode (supply rate of magma and the external water; Wohletz and Sheridan 1983), as well as by the exact nature of the coolant (White 1996).

The lithological and stratigraphic variations shown by the deposits at El Golfo (Fig. 5) suggest that the different transport and depositional mechanisms that characterize them were a product of changes in the eruption dynamics caused by changes in the efficiency of the hydromagmatic fragmentation. This implies that the eruption responsible for the construction of this tuff cone was continuous but had several pulses in which different types of deposits were formed. According to the resulting facies associations described above and their interpretation in light of the mechanisms of fragmentation, transportation and deposition, we are able to distinguish five stages or pulses in the eruption of this volcano (Table 1).

The first stage (I) is represented by the lithofacies association G1 (Fig. 5, Table 1), which consists of deposits characterised by the effects of the high rate of direct suspension sedimentation that alternate with tractional deposition (depending on the deposition rate). The general aspect of this lithofacies, characterised by poor sorting with coarse-grained tephra (coarse lapilli) alternating with beds of coarse ash, along with large clasts and blocks up to 30 cm in diameter, reflects in general high-energy transport with changes in the rate of deposition. The trajectories of the ballistic impacts indicate north-to-south transportation. The large amount of accidental basaltic lithic clasts can be interpreted as a vent-opening episode that occurred during the initial stages of the subsurface hydrovolcanic explosions.

The second stage (II) corresponds predominantly to the emplacement of multiple pyroclastic surges with subordinate undulate ash-beds (lithofacies association G2) (Fig. 5, Table 1). The resulting deposits show characteristic planar bedding, which may be considered as an upper flow-regime bedform. Higher fragmentation efficiency is suggested by the abundance of ash matrix in these deposits. This suggests an increase in the energy of the explosions, probably associated with greater efficiency in the energy transfer during the hydromagmatic process. Similar deposits can be observed at Surtsey, Capelinhos and Capelas (Waters and Fisher 1971; Kokelaar 1983, 1986; Solgevik et al. 2007). The presence of a number of ballistic blocks up to 50 cm in diameter (Fig. 5) suggest episodes of higher explosive energy.

The third stage (III) of the eruption is reflected in the succession of deposits in the lithofacies association G3 (Fig. 5, Tab. 1), which represents a further change in the transportation and depositional conditions. This stage consists of beds confined to channels formed by an eroding current with an initial erosive phase followed by a depositional stage. The rest of the unit is interpreted as resulting from the deposition of turbulent pyroclastic surges with fluctuating velocity and particle concentration, as well as

episodes of high shear stress leading to the formation of undulate deposits. These deposits are similar to the ones described in Solgevik et al. (2007) and Cole et al. (2001). These features—by comparison with those of the previous stage—indicate that this stage was characterised by higher-energy transport related to episodes of higher explosive energy, which also generated bomb- and block-rich (up to 35 cm in diameter) horizons.

Stage four (IV) can be correlated with wet explosions (lithofacies association G4) (Fig. 5, Tab. 1) in which a remobilisation of material occurred due to an excess of water (e.g. Sohn and Chough 1992). Individual explosions could also have produced water-charged tephra jets that landed on the flanks of the growing cone and acted as a source of ready-to-move free water. The U-shaped channels might also be the result of topographic variability with particle deposition or erosion. The presence of antidunes, planar stratified and accretionary lapilli suggest a complex emplacement of pyroclastic density currents with continuous changes in transportation and depositional conditions. The presence in smaller proportions of bedforms with ripple-type geometries and slopes in the opposite direction to the propagation direction of the main pyroclastic surges (i.e. antidunes) suggests an important increase in the energy of the flow (Fisher and Schmincke 1984), whilst the dunes represent lower-flow-regime bedforms.

Stage five (V) corresponds to the lithofacies association G5 (Fig. 5, Tab. 1) and is characterised by deposits containing large dunes, accretionary lapilli, antidunes, and undulate and planar stratified facies. The duration of the pyroclastic surges that caused their deposition was probably very short, and there is no evidence that during flow emplacement the materials of the bedform were eroded and adapted to the new flow conditions. The lack of fine material, probably elutriated during the transport process, in the cross-bedded levels, indicates that the flows generating these dunes were gas-supported. However, the presence of a facies with accretionary lapilli in the deposits of this last stage suggests that occasionally there was a moderate amount of liquid water (or moisture) in the surges and/or eruption clouds from which they formed (e.g. Fisher and Schmincke 1984; Heiken and Wohletz 1985). As a surge moves laterally away from the vent, it loses heat, solids and momentum, resulting in a decreasing wavelength and amplitude of the cross-stratified surge deposits as the distance from the vent increases (e.g. Waters and Fisher 1971; Wohletz and Sheridan 1979; Sohn and Chough 1989). The loss of heat results in the condensation of steam, which explains the increase in wet features. The amount of water might thus be related to the dynamics of the flow rather than the changing eruption conditions. This hypothesis was first proposed by Wohletz and Sheridan (1983).

In summary, the diversity of emplacement mechanisms inferred and grain size distributions observed in the stratigraphic sequence indicates that the eruptive and emplacement

mechanisms were not constant during the eruptive episode that generated the tuff cone of El Golfo. A general increase in the explosive energy can be seen as one moves upwards in the pyroclastic succession, indicating possibly that there was a trend towards an optimum magma/water ratio in the second half of the eruption, which would have led to an increase in the energy-exchange efficiency and, consequently, in the magma fragmentation. This is illustrated by the progressive increase in the degree of fragmentation (i.e. decrease in grain size) and in the energy of the resulting pyroclastic surges, which was probably related to a progressive reduction in the amount of sea water entering the vent as the volcanic edifice was being built. However, there is no evidence of any Strombolian phase during the eruption, which would seem to imply that to the west the tuff cone remained open to the sea during the whole eruption sequence, even at its end when the eastern side of the edifice had reached around 60 m a.s.l. This might probably be due to the continuous partial collapse of part of the edifice. The absence of any significant volume of lithic clasts derived from the substrate (e.g. fragments of older lavas or fossil beaches) suggests that the eruption did not excavate deeply into the substrate, and so we can assume that the magma–water interaction occurred mostly at a very shallow depth or even at sea level and can discard the idea that water could have been drawn into the conduit from a subsurface aquifer.

Post-depositional processes

The irregular geometry of the different alteration zones suggests that some primary causes for the palagonitisation should have existed. This process may be almost contemporaneous to tuff deposition (e.g. Capelas, Capelinhos and Sao Roque tuff cones in Azores, Solgevik et al. 2007, Cole et al. 2001, Zanon et al. 2009; Sinker Butte Volcano in USA, Brand and White 2007). The fact that the materials that are in contact with the highest topographic surface are the least altered indicates that, during the late depositional stages, the pyroclastic materials retained a small amount of steam shortly after being deposited. By contrast, the materials located in the lower half of the sequence are more altered, which implies that at the moment of deposition they retained a greater proportion of water as steam. In these lower sections, the steam remained trapped for longer, which may be related to the fact that the accumulation of materials occurred very rapidly and thus prevented the steam from escaping. Thus, once covered by the successive pyroclastic surges, the deposits would have acted as an aquatard that could explain the different degree of alteration between the upper and lower parts of the sequence at El Golfo, despite the lack of any clear (eruptive) separation.

The presence of interstitial water in the lower part of the sequence of deposits is also shown by the existence of tephra-lips that affected the whole wall and which are associated

with circular compaction faults (Fig. 8). The palagonitisation induced high secondary resistance in the tuff, resulting in a stress response that changed from pseudo-plastic to pseudo-brittle in behaviour. As a consequence, the response to this oriented stress was the formation of fractures and an immediate failure. During these slides, the entire block behaved as a single rigid unit (but sufficiently plastic). It is important to note that the downdropped section in front of El Golfo (Fig. 4d) exhibits the same type of alteration as the rest of the edifice but with the addition of a chaotic structure due to the slumping process. This suggests that the main landslide occurred once the palagonitization processes had already started. However, as has been demonstrated in the case of the Surtsey eruption (Kokelaar 1983; Moore 1985), it is possible that slumps occurred during the construction of the volcanic edifice and that the material displaced towards the vent was re-ejected during subsequent explosions.

Hazard implications

El Golfo is a good example of a tuff cone demonstrating how a single eruption may produce a complex sequence of eruption styles and depositional processes. Nonetheless, an examination of this volcano sheds light on a number of important implications for hazard assessment when considered within the framework of the fissural volcanism present in the Canary Islands. After the construction and partial erosion of its edifice, another eruptive episode took place in the northern section of El Golfo (Fig. 2). Three craters were formed, and lavas and Strombolian pyroclasts were emitted (Fig. 4d). Despite not occurring during the same eruptive episode, the formation of these new edifices can be linked to the same NEE–SWW fracture system that originated the tuff cone at El Golfo. We can see here how a fissure-dominated system in which scoria and/or lava spatter cones form long chains exhibits very different styles of eruptions at the extremities of the fissure. Subaerial conditions changing to shallow submarine conditions allowed for the development of a hydrovolcanic landform in the area. Sea-level changes during the long time in which the overall fissure system was active (as shown by the presence of fossil beaches) may have led to the construction of a complex set of volcano types in this lowland area with contrasting eruption styles and, consequently, a variety of associated hazards. While a small lava spatter eruption may be manageable, a full tuff cone or maar eruption would cause havoc on a local scale and would have very different repercussions in terms of its potential hazards. Furthermore, the pyroclastic deposits at El Golfo are very rich in xenoliths, and the existence of these plutonic enclaves in the basalts of Lanzarote would seem to suggest that on occasions a rapid ascent of magma to the surface occurs. On Lanzarote and the other Canary Islands, this type of long-lived fissure-dominated volcanism incorporating contrasting

eruption styles is not uncommon and should be studied in more detail as a means of conducting appropriate hazard assessment for this area.

Conclusions

The tuff cone at El Golfo is an example of a coastal volcanic edifice caused by simple hydrovolcanic activity without any evidence of Strombolian phases. Interaction of water with magma, mostly at sea level, dominated the whole eruptive process. The lithological and stratigraphic features present in the deposits at El Golfo suggest that most were formed by deposition from turbulent pyroclastic surges. These characteristics, together with the type and distribution of the palagonitic alteration that affects part of the materials and the absence of hyaloclastites, suggest that they were emplaced in a subaerial environment. The growth of the tuff cone can be divided roughly into five stages on the basis of the resulting deposits and different corresponding eruption mechanisms inferred. A continuous change in the transport/depositional system is revealed, with a possible progressive increase in the energy-transfer efficiency from magma to water and, consequently, in the eruption explosivity and in the degree of fragmentation. This volcano forms part of a long-lived fissural system that reaches down to the coastal plains, along which several monogenetic cones showing a large diversity of eruptive styles have formed. It reminds us that eruption dynamics and associated hazards may differ considerably within the same volcanic system if external variables (e.g. the availability of water) change.

Acknowledgements This research was partially funded by CTM2009-05919-E/ANT. The authors are grateful to the Cabildo of Lanzarote and the National Park of Timanfaya for giving permission to undertake this research, and to Orlando Hernandez (Casa de Los Volcanes-Cabildo de Lanzarote) for his assistance with the logistics. We are also grateful to the Editor James White, the Associated Editor Thorvaldur Thordarson and the reviewers Danilo Palladino, Karoly Németh and Christopher Hamilton for their constructive reviews of this manuscript.

References

- Abdel-Monem A, Watkins ND, Gast PW (1972) Potassium-argon ages, volcanic stratigraphy, and geomagnetic polarity history of the Canary Islands; Tenerife, La Palma and Hierro. *Am J Sci* 272(9):805–825
- Araña V, Carracedo J (1978) Cañarian volcanoes: Gran Canaria. Editorial Rueda, Madrid:1–175
- Araña V, Hansen A, Martí J (1988) La caldera y el Pico de Vandama (Gran Canaria). *Boletín Geológico y Minero T XCIX-I*:47–58
- Amott RWC, Hand BM (1989) Bedforms, primary structures and grain fabric in the presence of suspended sediment rain. *J Sediment Petrol* 59:1062–1069
- Baker E, Massoth G, de Ronde C, Lupton J, McInnes B (2002) Observations and sampling of an ongoing subsurface eruption of Kavachi volcano, Solomon Islands. *Geology* 30(11):975–978
- Banda E, Dan̄obeitia JJ, Surin̄ach E, Ansoorge J (1981) Features of crustal structure under the Canary Islands. *Earth Planet Sci Lett* 55(1):11–24
- Belousov A, Belousova M (2001) Eruptive process, effects and deposits of the 1996 and the ancient basaltic phreatomagmatic eruptions in Karymskoye lake Kamchatka. Russia. *Spec Publ int Assoc Sediment* 30:35–60
- Brand BD, White CM (2007) Origin and stratigraphy of phreatomagmatic deposits at the Pleistocene Sinker Butte Volcano, Western Snake River Plain, Idaho. *J Volcanol Geotherm Res* 160(3–4):319–339
- Branney MJ, Kokelaar P (2002) Pyroclastic density currents and the sedimentation of ignimbrites. *Geological Society of London Memoirs*, p 150
- Cas RAF, Wright JV (1987) Volcanic successions, modern and ancient. A geological approach to processes products and successions. Chapman and Hall, London, 528 pp
- Chough SK, Sohn YK (1990) Depositional mechanics and sequences of base surges, Songaksan tuffring, Cheju Island, Korea. *Sedimentology* 37(6):1115–1135
- Clarke H, Troll VR, Carracedo JC (2009) Phreatomagmatic to Strombolian eruptive activity of basaltic cinder cones: Montaña Los Erales, Tenerife, Canary Islands. *J Volcanol Geotherm Res* 180(2–4):225–245
- Cole PD (1991) Migration direction of sand-wave structures in pyroclastic-surge deposits; implications for depositional processes. *Geology* 19(11):1108–1111
- Cole PD, Guest J, Duncan A, Pacheco J (2001) Capelinhos 1957–1958, Faial, Azores: deposits formed by an emergent surtseyan eruption. *Bull Volcanol* 63(2):204–220
- Cronin SJ, Bonte-Grapentin M, Nemeth K (2006) Samoa technical report—review of volcanic hazard maps for Savai'i and Upolu. EU-SOPAC, MUIR, Massey, New Zealand
- De La Nuez J, Alonso J, Quesada M, Macu M (1993) Edificios hidromagmáticos costeros de Tenerife (Islas Canarias). *Rev Soc Geol España* 6(1–2):47–59
- Dellino P, Isaia R, La Volpe L, Orsi G (2004a) Interaction between particles transported by fallout and surge in the deposits of the Agnano-Monte Spina eruption (Campi Flegrei, Southern Italy). *J Volcanol Geotherm Res* 133(1–4):193–210
- Dellino P, Isaia R, Veneruso M (2004b) Turbulent boundary layer shear flows as an approximation of base surges at Campi Flegrei (Southern Italy). *J Volcanol Geotherm Res* 133(1–4):211–228
- Druitt TH (1992) Emplacement of the 18 May 1980 lateral blast deposit ENE of Mount St. Helens, Washington. *Bull Volcanol* 54(7):554–572
- Druitt TH (1998) Pyroclastic density currents. In: Gilbert, J.S., Sparks, R.S.J. (eds.), *The physics of explosive volcanic eruptions*. *Geol Soc Spec Publ* 145:145–182
- Fisher RV (1977) Erosion by volcanic base-surge density currents: U-shaped channels. *Geol Soc Am Bull* 88(9):1287–1297
- Fisher RV, Schmincke HU (1984) *Pyroclastic rocks*. Springer-Verlag Inc, Berlin, p 474
- Freundt A, Bursik M (1998) Pyroclastic flow transport mechanisms. In: Freundt A, Rosi M (eds) *From magma to tephra, modeling physical processes of explosive volcanic eruptions*, vol 4. Elsevier Science, Amsterdam, pp 173–231
- Fuster JM, Cendrro A, Gastesi P, Ibarróla E, Ruiz JL (1968) *Geología y volcanología de las islas Canarias: Tenerife*. Instituto 'Lucas Mallada', CSIC, Madrid:218 pp
- Gudmundsson MT, Thordarson T, Höskuldsson Á, Larsen G, Björnsson H, Prata FJ, Oddsson B, Magnússon E, Högnadóttir T, Petersen GN, Hayward CL, Stevenson JA, Jónsdóttir I (2012) Ash generation and distribution from the April-May 2010 eruption of Eyjafjallajökull, Iceland. *Sci. Rep.* 2
- Heiken G, Wohletz K (1985) *Volcanic ash*. University of California Press, Berkeley, p 246

- Houghton BF, Hackett WR (1984) Strombolian and phreatomagmatic deposits of Ohakune craters, Ruapehu, New Zealand: a complex interaction between external water and rising basaltic magma. *J Volcanol Geotherm Res* 21(3–4):207–231
- Huppert HE (1998) Quantitative modelling of granular suspension flows. *Phil Trans R Soc Lond* 356:2471–2496
- (IMO) (Icelandic Meteorological Office) <http://en.vedur.is/earthquakes-and-volcanism/articles/nr/1884>
- Ingram RL (1954) Terminology for the thickness of stratification and parting units in sedimentary rocks. *Geol Soc Am Bull* 65(9):937–938
- Jude-Eton TC, Thordarson T, Gudmundsson MT, Oddsson B (2012) Dynamics, stratigraphy and proximal dispersal of supraglacial tephra during the ice-confined 2004 eruption at Grímsvötn Volcano, Iceland. *Bull Volcanol* 74(5):1057–1082
- Kieffer S, Sturtevant B (1986) Erosional furrows formed during the lateral blast at Mount St. Helens, May 18, 1980: indicators of longitudinal vortices in the boundary layer. *Abstr. Intl. Volcanol. Cong. New Zealand* 53
- Kienle J, Kyle PR, Self S, Motyka RJ, Lorenz V (1980) Ukinrek Maars, Alaska, I. April 1977 eruption sequence, petrology and tectonic setting. *J Volcanol Geotherm Res* 7(1–2):11–37
- Kokelaar BP (1983) The mechanism of surtseyan volcanism. *J Geol Soc* 140(6):939–944
- Kokelaar BP (1986) Magma–water interactions in subaqueous and emergent basaltic volcanism. *Bull Volcanol* 48:275–289
- Larsen G (2010) 3 Katla: Tephrochronology and eruption history. In: Anders Schomacker JK, Kurt HK (eds) *Developments in Quaternary sciences*. Elsevier, pp 23–49
- Larsen G, Guðmundsson M, Sigmarsson O (2009) Katla. In: Sólnes J et al (eds) *Náttúruvía á Íslandi-Tekist á við náttúruöflin í 1100 ár. Eldgosavá. Viðlagatýgging Íslands, Reykjavík*
- Le Bas MJ, Rex DC, Stillman CJ (1986) The early magmatic chronology of Fuerteventura, Canary Islands. *Geol Mag* 123:287–298
- Lorenz V (1974a) Studies of the Surtsey tephra deposits. *Surtsey Res Prog Rep* 7:72–79
- Lorenz V (1974b) Vesiculated tuffs and associated features. *Sedimentology* 21:273–291
- Macdonald GA (1972) *Volcanoes*. Prentice-Hall, Inc, N.J., p 510
- Machado F, Parsons WH, Richards AF, Mulford JW (1962) Capelinhos eruption of Fayal Volcano, Azores, 1957–1958. *J Geophys Res* 67(9):3519–3529
- Marinoni LB, Gudmundsson A (2000) Dykes, faults and palaeostresses in the Teno and Anaga massifs of Tenerife (Canary Islands). *J Volcanol Geotherm Res* 103(1–4):83–103
- Marinoni LB, Pasquarè G (1994) Tectonic evolution of the emergent part of a volcanic ocean island: Lanzarote, Canary Islands. *Tectonophysics* 239(1–4):111–137
- Martí J, Colombo F (1990) Estratigrafía, sedimentología y mecanismos eruptivos del edificio hidromagmático de El Golfo (Lanzarote). *Bol Geol Min* 101(4):560–579
- Mastin LG, Christiansen RL, Thornber C, Lowenstern J, Beeson M (2004) What makes hydromagmatic eruptions violent? Some insights from the Keanakāko'i Ash, Kīlauea Volcano, Hawai'i. *J Volcanol Geotherm Res* 137(1–3):15–31
- Middleton G, Southard J (1978) Mechanics of sediment movement. *Soc Econ Paleontol Mineral Short Course 3, Eastern Section*: pp 6.37–36.41
- Moore J (1967) Base surge in recent volcanic eruptions. *Bull Volcanol* 30(1):337–363
- Moore JG (1985) Structures and eruptive mechanisms at Surtsey Volcano, Iceland. *Geol mag* 122(6):649–661
- Moore JG, Nakamura K, Alcaraz A (1966) The 1965 eruption of Taal Volcano. *Science* 151(3713):955–960
- Morimoto R (1960) Submarine eruption of the Myōjin reef. *Bull Volcanol* 23(1):151–160
- Németh K, Cronin SJ (2009) Volcanic structures and oral traditions of volcanism of Western Samoa (SW Pacific) and their implications for hazard education. *J Volcanol Geotherm Res* 186(3–4):223–237
- Németh K, Cronin SJ (2011) Drivers of explosivity and elevated hazard in basaltic fissure eruptions: the 1913 eruption of Ambrym Volcano, Vanuatu (SW-Pacific). *J Volcanol Geotherm Res* 201(1–4):194–209
- Robertson AHE, Stillman CJ (1979) Late Mesozoic sedimentary rocks of Fuerteventura, Canary Islands: implications for West African continental margin evolution. *J Geol Soc* 136(1):47–60
- Schumacher R, Schmincke HU (1991) Internal structure and occurrence of accretionary lapilli—a case study at Laacher See Volcano. *Bull Volcanol* 53(8):612–634
- Schumacher R, Schmincke HU (1995) Models for the origin of accretionary lapilli. *Bull Volcanol* 56(8):626–639
- Self S, Sparks R (1978) Characteristics of widespread pyroclastic deposits formed by the interaction of silicic magma and water. *Bull Volcanol* 41(3):196–212
- Self S, Kienle J, Huot J-P (1980) Ukinrek Maars, Alaska, II. Deposits and formation of the 1977 craters. *J Volcanol Geotherm Res* 7(1–2):39–65
- Sheridan MF, Wohletz KH (1981) Hydrovolcanic explosions: the systematics of water-pyroclast equilibration. *Science* 212:1387–1389
- Sheridan MF, Wohletz KH (1983) Hydrovolcanism: basic considerations and review. *J Volcanol Geotherm Res* 17(1–4):1–29
- Sohn YK (1996) Hydrovolcanic processes forming basaltic tuff rings and cones on Jeju Island, Korea. *Geol Soc Am Bull* 108:1199–1211
- Sohn YK, Chough SK (1989) Depositional processes of the Suwolbong tuff ring, Cheju Island (Korea). *Sedimentology* 36(5):837–855
- Sohn YK, Chough SK (1992) The Ilchulbong tuff cone, Cheju Island, South Korea: depositional processes and evolution of an emergent, surtseyan-type tuff cone. *Sedimentology* 39:523–544
- Sohn YK, Park JB, Khim BK, Park KH, Koh GW (2003) Stratigraphy, petrochemistry and Quaternary depositional record of the Songaksan tuff ring, Jeju Island, Korea. *J Volcanol Geotherm Res* 119(1–4):1–20
- Solgevik H, Mattsson HB, Hermelin O (2007) Growth of an emergent tuff cone: fragmentation and depositional processes recorded in the Capelas tuff cone, São Miguel, Azores. *J Volcanol Geotherm Res* 159(1):246–266
- Sumner JM (1998) Formation of clastogenic lava flows during fissure eruption and scoria cone collapse: the 1986 eruption of Izu-Oshima Volcano, eastern Japan. *Bull Volcanol* 60(3):195–212
- Thorarinsson S (1965) The Surtsey eruption: course of events and development of the new island. *Surtsey Res Prog Rep* 1:51–55
- Valentine GA (1987) Stratified flow in pyroclastic surges. *Bull Volcanol* 49(4):616–630
- Valentine GA, Fisher RV (2000) Pyroclastic surges and blasts. In: Sigurdsson, H., Houghton, B.F., McNutt, S.R., Rymer, H., Stix, J. (Eds.), *Encyclopedia of volcanoes*. New York, Academic Press: 571–580
- Verwoerd WJ, Chevallier L (1987) Contrasting types of surtseyan tuff cones on Marion and Prince Edward islands, southwest Indian Ocean. *Bull Volcanol* 49(1):399–413
- Waitt RB, Dzurisin D (1981) Devastating pyroclastic density flow and attendant air fall of May 18—Stratigraphy and sedimentology deposits. In: *The 1980 eruptions of Mount St. Helens, Washington* (ed. by P.W. Lipman & D.R. Mullineaux), *Pap. US Geol. Surv.* 1250 439–458
- Walker GPL (1984) Characteristics of dune-bedded pyroclastic surge bedsets. *J Volcanol Geotherm Res* 20(3–4):281–296
- Waters AC, Fisher RV (1971) Base surges and their deposits: Capelinhos and Taal volcanoes. *J Geophys Res* 76(23):5596–5614
- White JDL (1996) Impure coolants and interaction dynamics of phreatomagmatic eruptions. *J Volcanol Geotherm Res* 74(3–4):155–170
- White JDL, Houghton B (2000) Surtseyan and related phreatomagmatic eruptions. In: Sigurdsson H, Houghton BF, McNutt SR, Rymer H,

- Stix J (eds) *Encyclopedia of volcanoes*. Academic Press, 511, p 495
- White JDL, Ross PS (2011) Maar-diatreme volcanoes: a review. *J Volcanol Geotherm Res* 201(1–4):1–29
- White JDL, Schmincke H-U (1999) Phreatomagmatic eruptive and depositional processes during the 1949 eruption on La Palma (Canary Islands). *J Volcanol Geotherm Res* 94(1–4):283–304
- Wohletz KH, Sheridan MF (1979) A model of pyroclastic surge. In: Chapin, C.E., Elston, W.E. (eds.). *Geol Soc Am Spec Pap* 180:177–194
- Wohletz KH, Sheridan MF (1983) Hydrovolcanic explosions; II, Evolution of basaltic tuff rings and tuff cones. *Am J Sci* 283(5):385–413
- Wohletz KH (1998) Pyroclastic surges and compressible two-phase flow. In: Freundt A, Rosi M (eds) *From magma to tephra: modelling physical processes of explosive volcanic eruptions*. Elsevier, Amsterdam
- Zanon V, Pacheco J, Pimentel A (2009) Growth and evolution of an emergent tuff cone: considerations from structural geology, geomorphology and facies analysis of São Roque volcano, São Miguel (Azores). *J Volcanol Geotherm Res* 180(2–4):277–291